

Influence of the ventricular folds on a voice source with specified vocal fold motion^{a)}

Richard S. McGowan^{b)}

CReSS LLC, 1 Seaborn Place, Lexington, Massachusetts 02420

Michael S. Howe

College of Engineering, Boston University, 110 Cummington Street, Boston, Massachusetts 02215

(Received 11 December 2008; revised 30 June 2009; accepted 2 July 2009)

The unsteady drag on the vocal folds is the major source of sound during voiced speech. The drag force is caused by vortex shedding from the vocal folds. The influence of the ventricular folds (i.e., the “false” vocal folds that protrude into the vocal tract a short distance downstream of the glottis) on the drag and the voice source are examined in this paper by means of a theoretical model involving vortex sheets in a two-dimensional geometry. The effect of the ventricular folds on the output acoustic pressure is found to be small when the movement of the vocal folds is prescribed. It is argued that the effect remains small when fluid-structure interactions account for vocal fold movement. These conclusions can be justified mathematically when the characteristic time scale for change in the velocity of the glottal jet is large compared to the time it takes for a vortex disturbance to be convected through the vocal fold and ventricular fold region.

© 2010 Acoustical Society of America. [DOI: 10.1121/1.3299200]

PACS number(s): 43.70.Bk, 43.70.Gr [DOS]

Pages: 1519–1527

I. INTRODUCTION

The larynx is a complex structure of muscle, cartilage, and epithelium where voiced sounds can be created. The vocal folds consist of a pair of layered structures that partially obstruct the flow produced when the lung pressure is somewhat greater than the pharyngeal pressure. Muscles adjust the positions of the folds to permit flow-structure interaction that drives the vocal folds into oscillation. These oscillations periodically change both the size of the region of air between the folds, known as the glottis, and the resistance to flow through the glottis (van den Berg *et al.*, 1957; Fant, 1960). The resistance to flow is equal and opposite to the drag experienced by the vocal folds, and the resulting fluctuations in the volume velocity of air into the vocal tract generate sound that is heard to emanate from the mouth (Titze, 1994; Stevens, 1998). The sound coming from the laryngeal region can be viewed as having been generated from a fluctuating drag, or pressure expansion waves, superposed on an otherwise uniform pressure wave traveling from the lungs (Zhao *et al.*, 2002; Howe and McGowan, 2007).

Howe and McGowan (2007) presented a theory of the voice source derived using an aeroacoustic analogy and the method of compact Green’s functions (Howe, 1975, 1998, 2003). They showed that the major source of sound, the fluctuating drag on the vocal folds, can be calculated with knowledge of the distribution of fluid velocity in regions where vorticity is nonzero, which can be idealized to be a very thin shear layer at the boundary between the glottal jet and the surrounding air in the vocal tract. The calculation of

the magnitude of the drag or, equivalently, the source’s effect on the output acoustics is localized to be within the shear layer just downstream of the glottal exit because of the shape of the vocal folds. The convolutive solution with a compact Green’s function makes explicit the required alignment between the fluid velocity field near the vocal folds and the shape of the vocal folds in order that there be nonzero drag. The effect of the shape of the vocal folds on tissue-air forces is expressed in a factor of the Green’s function known as the *Kirchhoff vector*. Because drag is the force of interest, it is the axial component of the Kirchhoff vector that is relevant. Roughly, the axial component of the Kirchhoff vector for the vocal folds is the velocity potential field with unit inflow and outflow in the direction of the vocal tract axis—it depends only on the shape of the tissue boundaries. This potential flow has a stream function, which is here termed the *axial Kirchhoff stream function*. Figure 1(a) shows model vocal folds and Fig. 1(b) shows the axial Kirchhoff streamlines, on which the axial Kirchhoff stream function is constant, below the vocal tract axis of symmetry. At the glottal exit region the gradient of axial Kirchhoff stream function has a large component parallel to the glottal jet velocity; this is a necessary condition for the generation of drag between the tissue and air (e.g., Howe, 1998, 2003).

Howe and McGowan (2007) based their analysis on a relatively simple geometry in order to derive drag on the vocal folds: vocal folds in a uniform duct. The present paper extends that account to tissue structure just downstream of the vocal folds, known as the ventricular folds, or false vocal folds. Like the vocal folds, they protrude into the vocal tract at a distance generally less than 1 cm from the downstream end of the vocal folds (Agarwal *et al.*, 2003). The streamlines of the axial component Kirchhoff vector will certainly

^{a)}This paper is based on work presented at the 6th ICVPB, Tampere, Finland, 6–9 August 2008.

^{b)}Author to whom correspondence should be addressed. Electronic mail: rsmcgowan@cressllc.net

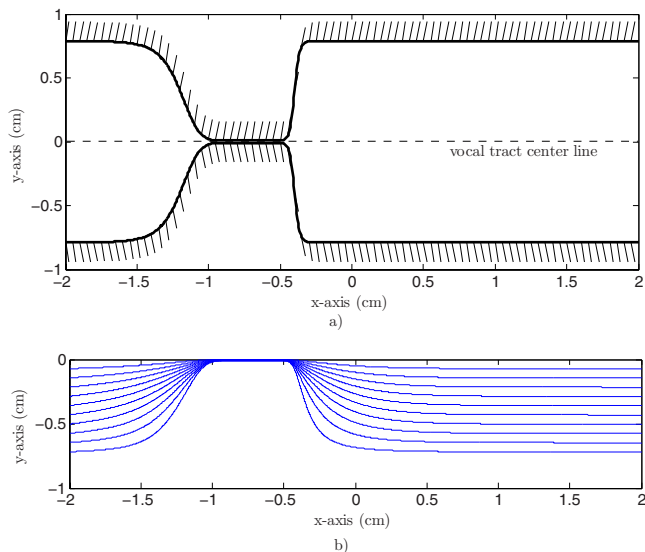


FIG. 1. (Color online) (a) Model vocal folds in the midsagittal plane and (b) axial Kirchhoff stream function streamlines below the axis of symmetry.

be altered near the ventricular folds compared to when they are assumed to be absent. Further, the ventricular folds are proximate enough to the vocal folds that the streamline patterns near the glottal exit can be expected to be altered as well. Either can produce change in the overall force between the tissues and the air near the vocal folds and, thus, affect the radiated acoustic field.

Zhang *et al.* (2002) provided a calculation of the effect of the ventricular folds on the voice source based on computational fluid dynamics (CFD). They found little effect of the ventricular folds on the voice source below 2000 Hz. Routine use of CFD can be very expensive and time-consuming, and, thus, it is difficult to confirm predictions for many possible fundamental frequencies and ventricular fold shapes. The approach of this paper is to generalize the analytic results of Howe and McGowan (2007) to include obstructions close to the vocal folds, which also requires some computational work, but at a much lower effort than full scale CFD.

The movement of the vocal folds will be specified by a simple mathematical model, and the ventricular folds are assumed to be rigid. This kind of analysis is employed when the effects of changes in fluid mechanics are considered without the complications of changes in vibrational patterns caused by fluid-structure interaction (e.g., Zhang *et al.*, 2002). These interactions are a part of the aerodynamic-myoelectric theory of vocal fold vibration. Therefore the results of our study are limited to the determination of the effect of the ventricular folds on the air flow itself, without quantitative consideration on how the ventricular folds influence the vibration of the vocal folds. Section II reviews some of the basic theory from Howe and McGowan (2007) and concludes with an equation for calculation of the drag if structures close to the vocal folds are included. Section III introduces the approximations used in the numerical calculation of the output pressure variation with and without ventricular folds. Section IV presents the results of these calculations, showing that the ventricular folds are expected to have a small effect on the propagated pressure wave from the

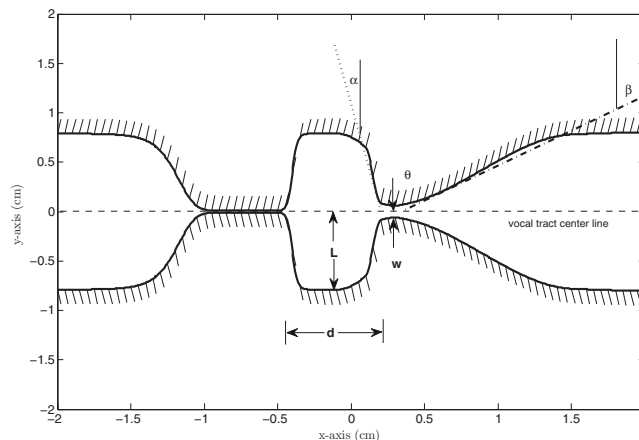


FIG. 2. Model vocal folds and ventricular folds in the midsagittal plane.

glottis at frequencies below 2 kHz. In Sec. V it is shown that this is the expected result given the behavior of the axial component of the Kirchhoff vector and the quasi-steady nature of the low-frequency portions of the glottal velocity pulse.

II. THEORETICAL BACKGROUND

The geometries of concern are illustrated in Figs. 1(a) and 2. In Fig. 1(a) the vocal folds form a constriction, the glottis, and in Fig. 2 vocal folds are shown forming a constriction to the left (upstream), and the ventricular folds form a secondary constriction to the right (downstream) in a rigid duct of uniform width $2h$. The figures show a two-dimensional geometry in the x - y plane, with the z direction orthogonal to this plane. The x -axis is the duct centerline and it denotes the axial direction. The coordinate system origin is taken to be about 0.4 cm downstream from the glottis in its rest state. The distance between the downstream end of the vocal folds and ventricular fold constriction is of the order of 1 cm, and, together, these structures occupy less than 4 cm of the vocal tract axis. The source region including both structures can therefore be considered to be acoustically compact for frequencies below about 5 kHz. Only plane wave propagation is assumed to occur in the duct.

Peak air speeds in the glottis during phonation at a conversational level should be less than 4000 cm/s. Assuming that the amount of heat created by viscous action in the vocal tract is small and body temperature does not vary substantially, the flow can be considered to be homentropic. Howe's (1998) formulation of Lighthill's (1952) equation for the production and propagation of sound at low Mach number flow that may be considered homentropic is

$$\left(\frac{1}{c_o^2} \frac{\partial^2}{\partial t^2} - \nabla^2 \right) B = \text{div}(\boldsymbol{\omega} \wedge \mathbf{v}), \quad (1)$$

where c_o is the mean speed of sound, which is approximately uniform and constant in low speed flows, and B is the *total enthalpy* defined in homentropic flow by

$$B = \int \frac{dp}{\rho} + \frac{1}{2} v^2, \quad (2)$$

where $v=|\mathbf{v}|$, \mathbf{v} is the fluid velocity, $\boldsymbol{\omega}=\text{curl}\mathbf{v}$, the vorticity, and $\rho\equiv\rho(p)$ is the density.

Let the incident over-pressure from the lungs consist of a step rise in pressure of amplitude p_I impinging on the glottis at $t=0$. Then the corresponding incident total enthalpy wave B_I can be written as

$$B_I=B_I\left(t-\frac{x}{c_o}\right)=\frac{p_I}{\rho_o}H\left(t-\frac{x}{c_o}\right), \quad (3)$$

where H is the Heaviside step function. Put $B=B_I+B_s$, where B_s is the field scattered at the vocal folds, and the ventricular folds if they are present, which has outgoing wave behavior at large distances from the glottis.

Howe and McGowan (2007) derived the following integral representation of the solution to Eqs. (1) and (3):

$$\begin{aligned} B(\mathbf{x},t) &= \frac{p_I}{\rho_o} \left\{ H\left(t-\frac{x}{c_o}\right) \right. \\ &\quad \left. - \frac{\text{sgn}(x)}{\ell([t])} \int_{-\infty}^{[t]} \frac{\partial}{\partial\tau} (H(\tau)\ell(\tau)) e^{-\int_{\tau}^{[t]} 2c_o d\xi \ell(\xi)} d\tau \right\} \\ &\quad - \int [(\boldsymbol{\omega} \wedge \mathbf{v})(\mathbf{y},\tau)] \cdot [\nabla_{\mathbf{y}} G(\mathbf{x},\mathbf{y},t,\tau)] d^3\mathbf{y} d\tau \\ &\quad + \oint_{S(\mathbf{y},\tau)} G(\mathbf{x},\mathbf{y},t,\tau) \left[\frac{\partial\mathbf{v}}{\partial\tau}(\mathbf{y},\tau) \right] \cdot d\mathbf{S}(\mathbf{y}) d\tau, \quad (4) \end{aligned}$$

where G is the acoustic Green's function associated with the geometry of either Fig. 1(a) or Fig. 2, $[t]=t-|x|/c_o$ is the acoustic delay time, and viscous terms have been neglected, which is valid for high Reynolds number flows, and thus, for all times except possibly when the vocal folds are nearly closed. $\ell(t)$ is the time-dependent Rayleigh "end correction" of the glottal constriction and ventricular fold constriction, if it exists (Rayleigh, 1945). [Note that unprimed coordinates will be associated with the field coordinate vector \mathbf{x} and primed coordinates with the source coordinate vector \mathbf{y} . Thus, $\mathbf{x}=(x,y,z)$ and $\mathbf{y}=(x',y',z')$.]

Let Y be the axial Kirchhoff vector at time t for either the geometry without ventricular folds [Fig. 1(a)] or with ventricular folds (Fig. 2). It is a solution of Laplace's equation satisfying $\partial Y/\partial x'_n=0$ on the surfaces $S(t)$ of the folds and the duct walls, and can be normalized such that

$$Y \sim x' \pm \frac{\ell(t)}{2}, \quad x' \rightarrow \pm \infty. \quad (5)$$

The end correction is given by

$$\ell(t) = \int_{-\infty}^{\infty} \left(\frac{\partial Y}{\partial x'}(\mathbf{y},t) - 1 \right) dx', \quad (6)$$

provided the duct cross-sections are the same on both sides of the region containing the vocal folds and ventricular folds, if they exist. The integration is along any path parallel to the duct axis passing through the constriction(s).

The method of compact Green's function was used to derive an approximation to the Green's function appearing in

Eq. (4) (Howe and McGowan, 2007). The compact approximation to the Green's function for source positions in the vicinity of the constrictions, $\mathbf{y} \sim h$, is

$$\begin{aligned} G(\mathbf{x},\mathbf{y},t,\tau) &\approx \frac{c_o}{2\mathcal{A}} H([t]-\tau) + \frac{c_o \text{sgn}(x) Y(\mathbf{y},\tau)}{\ell([t])\mathcal{A}} \\ &\quad \times H([t]-\tau) e^{-\int_{\tau}^{[t]} 2c_o d\xi \ell(\xi)}, \quad \mathbf{y} \sim O(h), \quad (7) \end{aligned}$$

where $\mathcal{A}=2h\ell_3$ is the cross-sectional area of the duct and ℓ_3 is the length in the z -dimension. The differences between Green's function in a geometry without ventricular folds [Fig. 1(a)] and a geometry with ventricular folds (Fig. 2) are governed by the corresponding differences in the axial component of the Kirchhoff vector Y .

The first term of Eq. (4) is the incident pressure wave, the second term is the initial transient response, the third term is the vortex sound source or drag term, and the fourth term represents the sound created by changes in the volume of the vocal folds. In this paper we are concerned with the evaluation of the vortex sound when ventricular folds are placed just downstream of the vocal folds. The fourth term, which is the monopole strength caused by unsteady volume change, will not be considered further because the absence or presence of the ventricular folds has no effect on this term.

After the step wave of pressure given in Eq. (3) reaches the vocal folds, vorticity is shed from the vocal folds and it is convected downstream in jet shear layers. The strength of the vorticity shed from the vocal folds depends on the relative velocity between the jet and the air outside the jet and, to a first approximation, is proportional to the velocity of the jet. Further, neglecting the effects of viscous dissipation, the circulation of each vortex element of the shed vorticity remains constant as it is convected downstream. The typical approximation is that the shear layer vorticity convects at one-half the local jet velocity that is associated with its circulation. Vortex sound is directly related to the fluctuating drag on the structures in the duct (i.e., forces on structures directed along the axis of the duct).

If the far-field (i.e., typically at a distance from the source region exceeding a duct diameter) is considered and the contribution from the fluctuating volume term (the fourth term on the right) in Eq. (4) is excluded, $B(\mathbf{x},t) \approx p'(x,t)/\rho_o$, where the prime denotes the pressure field without the monopole term. For $x>0$ the acoustic particle velocity of this outgoing wave is equal to $p'(x,t)/\rho_o c_o$. Let

$$U(t) = \lim_{x \rightarrow +0} \frac{p'(x,t)}{\rho_o c_o} \quad (8)$$

be the limiting value of this velocity just to the right of the vocal fold region in Fig. 1(a) or the vocal fold and ventricular fold region in Fig. 2. Also, $x \sim +0$ so that $[t] \rightarrow t$. In this limit, an equation for $U(t)$ can be derived in the form

$$\frac{d(\ell U)}{dt} + 2c_o U + B_\omega = \frac{2p_I}{\rho_o} H(t), \quad (9)$$

with

$$B_\omega = \int [(\boldsymbol{\omega} \wedge \mathbf{v})(\mathbf{y}, \tau)] \cdot [\nabla_y G(\mathbf{x}, \mathbf{y}, t, \tau)] d^3 y d\tau, \quad (10)$$

where B_ω is the vortex sound term from Eq. (4). Equation (9) is a modification of one found in [Howe and McGowan, 2007](#) [Eq. 6.3] with B_ω left unevaluated so that the effect of geometric changes in the laryngeal region, especially the inclusion of ventricular folds, can be studied. In [Howe and McGowan, 2007](#) B_ω was evaluated in terms of jet velocity using the fact that the jet was narrow compared to the width of the duct and without further obstructions downstream. With the addition of ventricular folds, a numerical procedure is necessary to evaluate this integral.

III. METHOD

A. Vocal folds and ventricular folds

The effect of the ventricular folds on the acoustic output was determined by solving Eqs. (9) and (10) numerically. The geometry of the vocal folds was based on a model for the vocal folds given by [Zhao et al. \(2002\)](#). The model for the vocal fold movement had two-dimensional symmetry and was adapted from the original cylindrical geometry ([Howe and McGowan, 2007](#)). A further modification was made here so that the folds were narrower in the axial direction and the faces of the vocal folds were steeper, to make them accord with known dimensions. Let $\Delta(x, t)$ be the distance between the vocal folds, so that

$$\Delta(x, t) = \frac{1}{2}(D_0 + D_{\min} + (D_0 - D_{\min})\tanh(\hat{s})) + D_{\max}[1 - \tanh(\hat{s})][(\hat{x} + \hat{c})\beta_1(T) - (\hat{x} - \hat{c})\beta_2(T)], \quad (11)$$

where $T = f_o t - [f_o t]$ is the fractional part of $f_o t$, and where

$$\hat{s} = \hat{b} \left(\left| \hat{x} \right| - \frac{1}{|\hat{x}|} \right),$$

$$\hat{x} = \frac{x + 0.8}{D_{\max}},$$

$$\hat{b} = \begin{cases} 1.4 & \text{if } \hat{x} < 0 \\ 6.0 & \text{otherwise,} \end{cases}$$

$$\hat{c} = 0.42,$$

$$\beta_1(T) = \begin{cases} 0 & \text{if } T \leq \frac{1}{9} \\ 0.244 \left\{ 1 - \cos \left[\frac{9\pi}{4} \left(T - \frac{1}{9} \right) \right] \right\} & \text{if } \frac{1}{9} < T \leq \frac{5}{9} \\ 0.488 & \text{if } \frac{5}{9} < T \leq \frac{6}{9} \\ 0.244 \left\{ 1 + \cos \left[3\pi \left(T - \frac{6}{9} \right) \right] \right\} & \text{if } \frac{6}{9} < T \leq 1, \end{cases}$$

$$\beta_2(T) = \beta_1\left(T + \frac{1}{9}\right),$$

$\Delta_0 = h$, $D_{\min} = 0.02$ cm, and $D_{\max} = 0.2$ cm. With these parameters the minimum glottal width $\Delta_m(t)$ varied from 0.015 to 0.1 cm.

Data provided in [Agarwal et al., 2003](#) were used to guide the choice of the dimensions of the ventricular folds and their position relative to the vocal folds for the numerical experiments. These measures were taken from laminagraphic images while subjects phonated, and those used in this study are illustrated in Fig. 2. The only modification to the dimensions of [Agarwal et al. \(2003\)](#) was to make the distance between the ventricular folds smaller than measured. It is possible for human speakers to reduce this distance, and we wanted to maximize the possibility that the ventricular folds could have any effect on the output acoustics. All of the measured values refer to [Agarwal et al. \(2003\)](#). The gap between the ventricular folds in measurements was between 0.2 and 0.8 cm, so the distance from a ventricular fold to the vocal tract axis w was measured to be between 0.1 and 0.4 cm. We have taken the distance w to be 0.06 cm in this work, which meant that the height of the lower vocal fold at minimum fold separation was only 0.01 cm higher than the lower ventricular fold when the glottis was maximally open. The measured distance d from the downstream edge of the vocal folds to the false folds ranged from 0.2 to 0.75 cm, and the distance used here was 0.7 cm. The measured maximum width of the channel between the ventricular sinuses ranged from 0.9 to 2.3 cm, and, thus, the maximum distance L from the bottom of one ventricular sinus to the vocal tract axis was between 0.45 and 1.15 cm, while $L = 0.8$ cm here. (The ventricular sinus is the gap downstream of the vocal folds and upstream of the ventricular folds.) The measured interior angle of the lines tangent to the downstream face and upstream face of the ventricular folds θ ranged between 55° and 107° . In this paper we let $\theta = 80^\circ$. The angle α between the tangent of the upstream ventricular fold surface and the perpendicular to the vocal tract axis was measured to be between -18° and 51° , and $\alpha = 15^\circ$ in this paper. Finally the measured angle between the tangent of the downstream ventricular fold surface and the perpendicular to the vocal tract axis β was between 22° and 76° , and $\beta = 65^\circ$ in this work.

B. Numerical method

All vorticity is represented by vortex lines that extend into the z direction. As these vortex lines originate on the vocal folds and are convected downstream, they form two continua that appear as curves in the x - y plane. These continua are vortex sheets in the limit of large Reynolds numbers. The two vortex sheets separate the glottal jet from the surrounding quiescent air in the rest of the duct.

The equation for Green's function, Eq. (7), can be used to simplify Eq. (10), the vortex sound term, in the limit $x \rightarrow +0$. In this limit the acoustic time delay is zero, and the time integral in Eq. (10) can be evaluated using an asymptotic approximation, so that the remaining spatial integral is evaluated at time t . Further, integrating in the z direction, Eq. (10) can be written in simplified form

$$B_\omega(\mathbf{x}, t) = \frac{1}{4h} \int \left[\omega \left(-v_{y'} \frac{\partial Y}{\partial x'} + v_{x'} \frac{\partial Y}{\partial y'} \right) \right] (\mathbf{y}, t) d^2\mathbf{y}, \quad (12)$$

where ω is the signed magnitude of vorticity, and $\mathbf{v} = v_{x'} \hat{\mathbf{i}} + v_{y'} \hat{\mathbf{j}}$ is the vorticity convection velocity.

In this two-dimensional geometry, the axial component of the Kirchhoff vector Y is the real part of a complex potential. The imaginary part is the corresponding axial Kirchhoff stream function ψ , say. Thus, Eq. (12) can be rewritten as

$$B_\omega = -\frac{1}{4h} \int [\omega(\mathbf{v} \cdot \nabla \psi)](\mathbf{y}, t) d^2\mathbf{y}. \quad (13)$$

Let $\mathbf{y}_\omega(t)$ be the position of the line vortex ω in the x - y plane. $\mathbf{y}_\omega(t) = \mathbf{y}_s(\tau_\omega) + \int_{\tau_\omega}^t \mathbf{v} dt'$, and τ_ω is the time that vortex ω is shed from the vocal fold surface at $\mathbf{y} = \mathbf{y}_s(\tau_\omega)$. Under the conditions of sufficiently low frequency, \mathbf{y}_ω describes two continuous, one-dimensional curves, within the region of the vocal and ventricular folds—one originating on the upper folds, $y'_s > 0$, denoted $\Omega^+ = \Omega^+(t)$, and the other from the lower folds, $y'_s < 0$, denoted $\Omega^- = \Omega^-(t)$. Let $s_\omega = s_\omega(t)$ be the distance along either vortex sheet from the shedding point at time t , and $s_\omega^\perp = s_\omega^\perp(t)$ be the distance measured from the outward normal to either vortex sheet. In a vortex sheet model,

$$\omega(s_\omega(t), t) = \pm U_\sigma(\tau_\omega) \delta(s_\omega^\perp(t)), \quad (14)$$

where $U_\sigma(t)$ is the asymptotic jet velocity predicted by free streamline theory and $\delta(\cdot)$ is the one-dimensional Dirac delta function. The plus sign in Eq. (14) corresponds to the vorticity shed from the upper vocal fold with $y'_s > 0$ and the minus sign to vorticity shed from the lower vocal fold with $y'_s < 0$. The magnitude of the convection velocity of the vorticity between the jet and surrounding fluid depends on the strength of the vorticity in terms of jet velocity U_σ , and the direction of convection is approximately the axial direction (x -axis).

$$\mathbf{v}(\mathbf{y}, t) = \frac{1}{2} U_\sigma(\tau_\omega) \hat{\mathbf{i}}. \quad (15)$$

Further, by symmetry, $\partial\psi/\partial x'((x', y'), t) = -\partial\psi/\partial x'((x', -y'), t)$. These considerations show that the contributions by each vortex sheet to the integral in Eq. (13) are equal, so that it is sufficient to consider the effect of the vortex sheet for $y'_s < 0$ in the integral and to double the result. The particle velocity in the jet is related to the particle velocity in the duct by mass conservation

$$U_\sigma(t) = \left(\frac{2h}{\sigma \Delta_m(t)} \right) U(t), \quad (16)$$

where σ is the jet contraction ratio.

Combining Eqs. (14)–(16), Eq. (13) can be rewritten as

$$B_\omega(t) = \frac{h}{2\sigma^2} \int_{\Omega^-} \left(\frac{U(\tau_\omega)}{\Delta_m(\tau_\omega)} \right)^2 \frac{\partial\psi}{\partial x'} ds_\omega. \quad (17)$$

It was shown in [Howe and McGowan \(2007\)](#) that the solution of the quasi-steady approximation to Eq. (9) [i.e., Eq. (9) with the time derivative term discarded] produced results

very close to the solution of the full equation. Substituting from Eq. (17) into the quasi-steady version of Eq. (9) and solving for $U(t)$ produce

$$U(t) \approx \frac{p_l H(t)}{\rho_0 c_0} \left(1 - \frac{\rho_0 h}{4p_l \sigma^2} \int_{\Omega^-} \left(\frac{U(\tau_\omega)}{\Delta_m(\tau_\omega)} \right)^2 \frac{\partial\psi}{\partial x'} ds_\omega \right). \quad (18)$$

A time step of $\Delta t = 0.00001$ s was used and the vortex sheet $\Omega^-(t)$ was approximated by discrete vortices shed at each time step. A fourth-order Runge–Kutta extrapolation was used to advance the positions of these discrete vortices. Then Eq. (18) was used to find the acoustic particle velocity at each time step, with a smoothing window that took a linear weighted average of the current value with the three previous values. The initial condition was $U(+0) = 0$. The integral in Eq. (18) was approximated using the trapezoid rule, with the term corresponding to $\tau_\omega = t$ excluded, as it had a negligible effect. The stream function ψ was found at each time step by solving Laplace's equation numerically with uniform inflow and outflow conditions at $x = -2$ cm and $x = 2$ cm. A standard second-order finite difference algorithm with a mesh of length 0.005 cm on each side was used for the potential flow solution.

The following were the values of the parameters appearing in this equation (all quantities are in c-g-s): $p_l = 8000$, $\rho_0 = 0.0013$, $h = 0.8$, $c_0 = 34800$, and $\ell_3 = 1$. The contraction ratio σ for vocal folds in high Reynolds number flow can be expected to be between 0.6 and 1.8 ([Park and Mongeau, 2007](#)), and its value was kept constant with the value unity. This is consistent with the assumption that the vorticity is convected in the x direction. Equation (11) was used to compute $\Delta_m(t)$ at each time step. The separation point $\mathbf{y}_s(t)$ was set to be the point on the surface of the vocal folds that was closest to the centerline of the duct, with one exception. The exception was when this entailed moving the separation point from the previous time step farther upstream than the distance that was traveled by the previously shed vortex in time Δt , in which case the separation point was set upstream from the previous point by that convection distance. Discontinuities in the vortex sheet were avoided by doing this. When the separation point moved downstream from the previous time step all the previously shed vortices that were upstream were presumed to reattach into the boundary layer.

Initially, numerical experiments were conducted at various fundamental frequencies f_0 and for various ventricular fold shapes. It became apparent that the effect of the ventricular folds on the outgoing acoustic particle velocity was small within the ranges of geometric parameters provided in [Agarwal et al. \(2003\)](#). The effect appeared to be largest when the ventricular folds were close together and the fundamental frequency was relatively high. Therefore, only one geometric condition with ventricular folds as previously described and shown in Fig. 2 will be examined below at relatively high f_0 s of 325 and 650 Hz.

IV. RESULTS

The acoustic signal downstream to the source region was computed using Eq. (18). The results are presented in terms of transmitted pressure, normalized by the subglottal

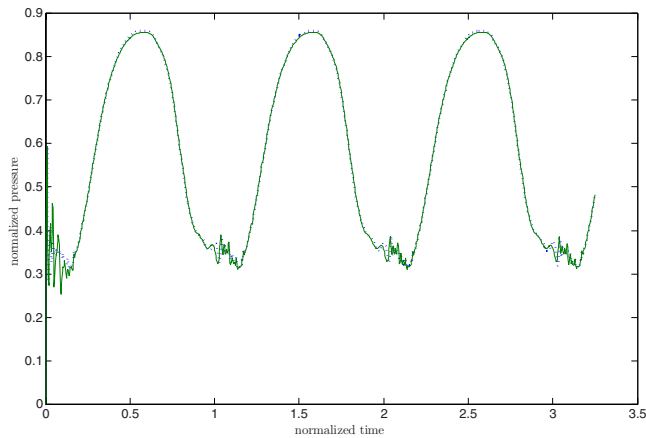


FIG. 3. (Color online) Propagated pressure wave downstream of the source region for when there are only vocal folds (dashed line) and when there are both vocal folds and ventricular folds (solid line) at $f_0=325$ Hz. Pressure is normalized by incident subglottal pressure p_l and time by $1/f_0$.

pressure in Figs. 3 and 4. Figure 3 compares the configuration with only vocal folds (dotted curve) to the configuration with ventricular folds added (solid curve) at $f_0=325$ Hz. The ventricular folds cause only a very slight decrease in peak transmitted pressure. Figure 4 shows the comparison at $f_0=650$ Hz. Again, the effect of the ventricular folds is very small.

Figure 5 shows the differences in the axial Kirchhoff streamlines for the case without ventricular folds [Fig. 5(a)] and the case with ventricular folds [Fig. 5(b)] when the vocal folds are at their most open position [one-half way through the cycle as defined by Eq. (10)]. The vortex sheets one-half through the first cycle are also indicated. Figure 6 shows the gradient of ψ projected onto the vortex convection direction (the x direction), at the same phase of the glottal cycle shown in Fig. 5. Figure 6(a) is without ventricular folds and Fig. 6(b) is with ventricular folds.

Equation (18) involves integration along a vortex sheet, so it is important to be aware of its location and shape. Figure 7 shows the vortex sheet in steps of one-sixth of a cycle during the second cycle in the case of $f_0=325$ Hz with ventricular folds. Figure 8 shows the same sequence for f_0

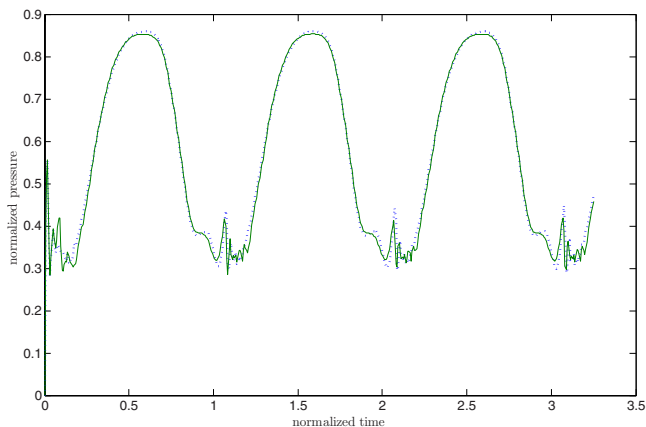


FIG. 4. (Color online) Propagated pressure wave downstream of the source region for when there are only vocal folds (dashed line) and when there are both vocal folds and ventricular folds (solid line) at $f_0=650$ Hz. Pressure is normalized by incident subglottal pressure p_l and time by $1/f_0$.

$=650$ Hz. The vortex sheet begins to bend over on itself in the first frame of the second glottal cycle in Fig. 7 and in the second frame in Fig. 8. At these times the glottis is in the process of opening, and the faster moving vortices that were shed when the glottis was the most constricted are catching up with the slower moving vortices that were shed when the glottis was the least constricted in the previous cycle. Because Figs. 7 and 8 have the abscissa in time normalized by the vocal fold vibration period, the bending of the vortex sheet occurs at about the same absolute time into the second cycle for both the 325 Hz case and the 650 Hz case. This can be expected because the vortex convection velocities follow very similar patterns. This follows by comparing Figs. 3 and 4 and relating vortex convection velocity to acoustic pressure using Eqs. (8), (14), and (15). The place where this bending occurs is farther upstream for the 650 Hz case because the slower moving vortices shed in the first cycle have not moved as far downstream in the second cycle as in the 325 Hz case.

V. DISCUSSION

The numerical results showing little effect of the ventricular folds on the acoustic output are indicative of two general theorems that follow immediately from Eq. (13). First, in a steady flow, and for vorticity ultimately convected in the horizontal x direction, B_ω depends only on the difference between value of the ψ streamline on which the vorticity arises and the value of the “end” ψ streamline, which is the streamline on which the vortex sheet approaches as $x' \rightarrow +\infty$. This follows from the facts that, for a steady flow, both ω and \mathbf{v} are constants in time along the vortex sheet, so that the integral in Eq. (13) has only the x -component of the ψ gradient in the integrand. A second theorem also holds under the same conditions of steady flow and ultimately horizontally convected vorticity: Changes in the shapes of the channel wall will not affect B_ω as long as the value of the streamline on which the vorticity arises and the value of where the vorticity “ends” are unchanged. In the numerical experiments performed in the present work, the streamlines from which vorticity arose (i.e., the streamline at the surface of the vocal fold) and the streamlines where the vorticity becomes parallel to the channel axis were the same with and without the presence of the ventricular folds. Note that these theorems do not depend on the exact path that the vorticity follows, only that the convection ultimately be in the x direction. So the assumption that the vorticity be convected axially is not critical to the conclusion that the ventricular folds do not have a large effect on acoustic output, at least if the vortex sheets do not strike the ventricular folds.

The flows here were not steady. However, these theorems remain approximately true for unsteady flow as long as vorticity traverses the regions of substantial nonzero x -component of the ψ gradient in a short time. Time of traversal is short if the strength of the vorticity entering the region of substantial nonzero x -component of the ψ gradient is nearly equal to the strength of the vorticity exiting this region. In the case of the vocal folds, this time should be short in relation to the inverse of the characteristic frequency

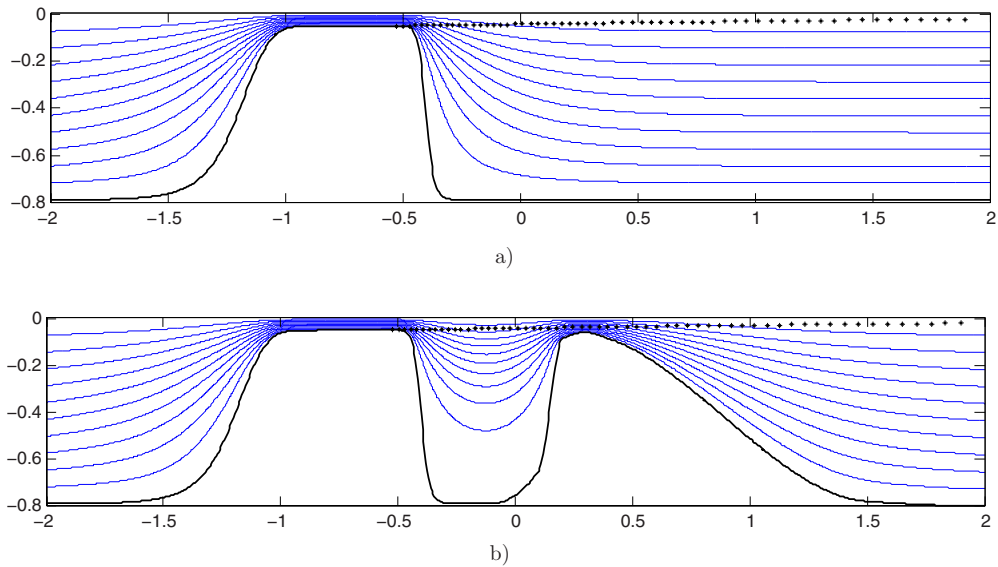


FIG. 5. (Color online) The streamlines of the horizontal component of the Kirchhoff vector and the vortex sheet at 1/2 of the vocal fold cycle, when the vocal folds are maximally open (a) for the case when there are only vocal folds and (b) for the case with ventricular folds.

of the variation in vortex strength. If d is the length scale of the region of substantial nonzero gradient, f_0 is a characteristic frequency for the variation of vortex strength, and V is the vorticity convection velocity in the same region, then the condition that $(f_0 d)/V \ll 1$ is necessary for each region of nonzero x -component of the ψ gradient. In the middle of the glottal cycle shown in Fig. 6(b), there is a region of substantial positive x -component of gradient at the trailing edge of the vocal folds, followed by a region of substantial negative

x -component of gradient before the leading edge of the ventricular folds, and a region of substantial positive x -component of gradient after the peak of the ventricular folds. The length scale for these regions together is of the order of 1.0 cm. The vortex convection velocities range from about 1500 to 2600 cm/s, so at 325 and 650 Hz $(f_0 d)/V$ is at most 0.4, and often much smaller.

Another way of interpreting the weak effect on voicing of the ventricular folds is as follows. Vorticity shed from the

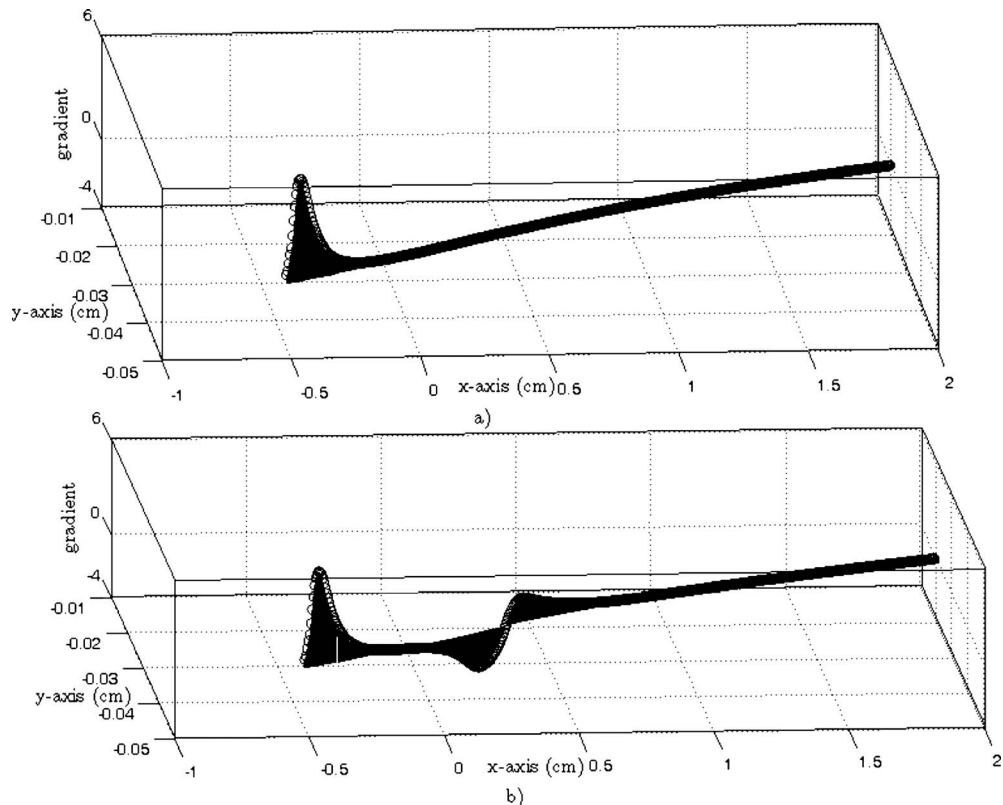


FIG. 6. Gradient of the axial Kirchhoff stream function projected onto the vortex convection direction (x -axis) as a function of position of the elements of the vortex sheet at 1/2 of the vocal fold cycle (a) for the case when there are only vocal folds and (b) for the case with ventricular folds.

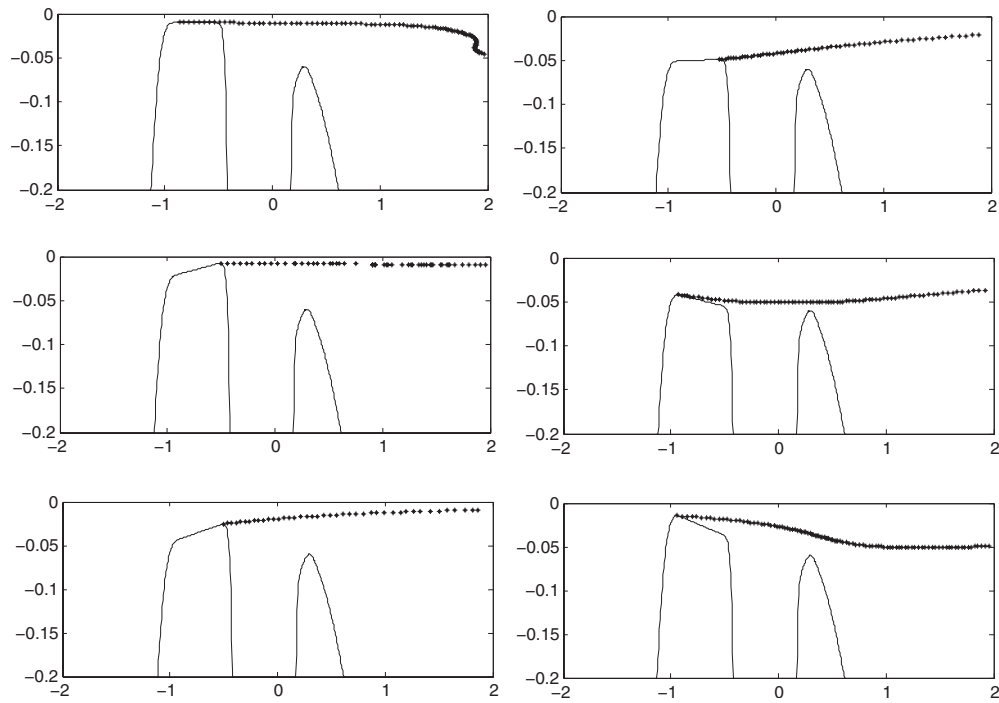


FIG. 7. Vortex sheet at $f_0=325$ Hz shown with outlines of the top of the vocal folds and the ventricular folds at $1/6$ intervals of the second glottal cycle. The columns of panels on the left are during the opening phase, sequenced from top to bottom. The columns on the right are during the closing phase, sequenced from top to bottom. The y -axis has been magnified with respect to the x -axis.

vocal folds always passes through the positive x -component of ψ gradient region, creating the fluctuating drag force that is propagated as sound down the vocal tract. The ventricular folds also create their own nonzero regions of x -component of gradient, strongest near the top of the ventricular folds, but with a negative and a positive x -component of gradient regions that tend to cancel one another.

Figures 7 and 8 indicate that the vortex sheets will eventually fold onto themselves. The higher the fundamental frequency, the farther upstream this folding will occur, as indicated by comparing the two figures. The folding is a prelude to transitions to the vortex sheet breaking apart and, eventually, a transition to turbulence. At frequencies somewhat higher than 650 Hz examined here, the vortex sheet could

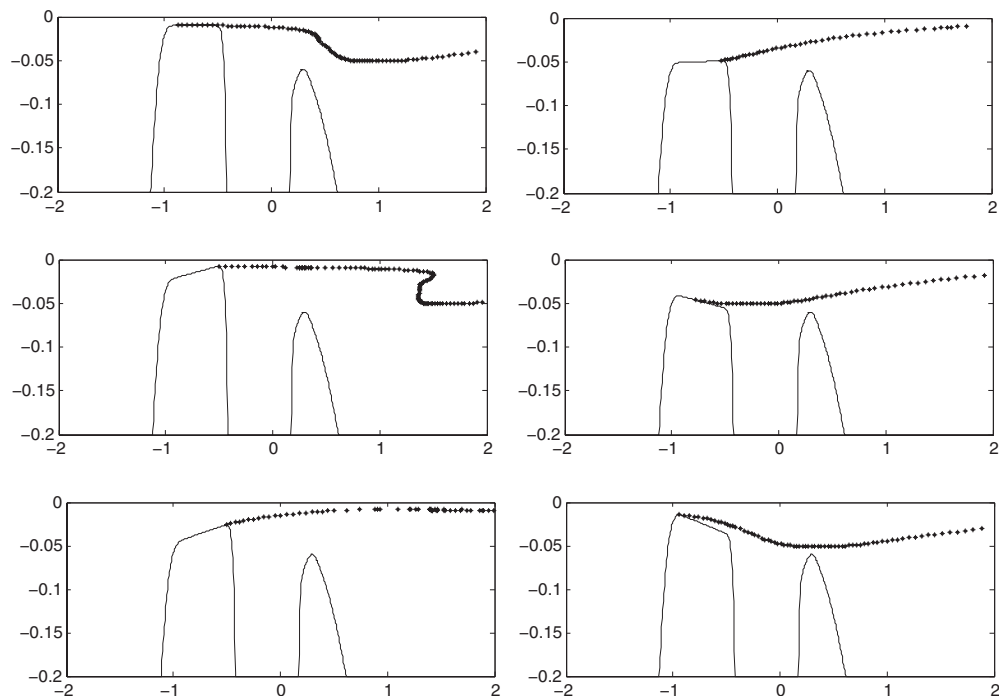


FIG. 8. Vortex sheet at $f_0=650$ Hz shown with outlines of the top of the vocal folds and the ventricular folds at $1/6$ intervals of the second glottal cycle. The columns of panels on the left are during the opening phase, sequenced from top to bottom. The columns on the right are during the closing phase, sequenced from top to bottom. The y -axis has been magnified with respect to the x -axis.

break up before passing above the tip of the ventricular folds. In this case the ventricular folds could have a substantial effect on the output acoustics farther down the vocal tract. The vorticity would interact with the negative x -component of the ψ gradient upstream of the ventricular folds in a coherent manner, but not with the positive gradient downstream. This would promote flow from the glottis because it would act as a negative resistance to flow, thus increasing the peak flow through the glottis. Thus the model is restricted to frequencies for which the vortex sheet does not break up before interacting with both the upstream and downstream sides of the ventricular folds. Further there is some experimental evidence that this kind of breakup can occur for nominally steady jets. Agarwal (2004) experimented with glottal jets and rigid model ventricular folds and found that the presence of the ventricular folds decreased the resistance to flow when the tips of the false folds were separated by distances from one to three times greater than the minimum distance between the vocal folds. This would indicate that the jets remained laminar from the glottis to the channel formed by the tips of the model false folds and became turbulent downstream of this channel. However, the intensity of the inflow turbulence and the level of noise downstream of the test section were not quantified in these experiments.

When vortex sheets' breakup occurs the condition that $(f_0 d)/V$ be small no longer holds, and new effects could be expected to be observed. One such effect is a positive feedback of the vorticity at the ventricular folds enhancing the vortex shedding in the glottis and, hence, the glottal jet. This effect is known as Rossiter buffeting (Howe, 1998) at frequencies greater than 2 kHz. Zhang *et al.* (2002) did attribute the occurrence of a peak in their predicted acoustic spectrum to this phenomenon in their CFD experiment. Whether this requires the breakup of the vortex sheet as described above, or only a time delay in interaction between upstream and downstream portions of the ventricular folds is uncertain at this time. The breaking up of the vortex sheet as described above would certainly enhance the buffeting.

Vortex sheet modeling has been used here on the basis that the distance through a glottal jet shear layer is negligible compared to other length scales, such as glottal channel width. This is a good approximation for the initial portion of the glottal jet. However, the jet shear layer thickens with downstream distance, and, depending on the height of the ventricular folds, a part of the jet will strike the upstream portion of the ventricular folds. This would add to the drag force, which appears to have been the case for false fold tips closer together than were the vocal fold surfaces in Agarwal's (2004) experiments.

VI. CONCLUSION

The ventricular folds do not have a noticeable effect on the voice source according to these results when the movement of the vocal folds is specified. This confirms the CFD results of Zhang *et al.* (2002) at low frequencies. This conclusion is derived from aeroacoustic theory and the use of compact Green's functions so that several fundamental frequencies and geometrical configurations are easily tested.

Most importantly, the numerical results can be confirmed by mathematical considerations regarding the integral of the gradient of the axial Kirchhoff stream function. This theoretical understanding is an important one for sources of sound in the vocal tract in general.

In a simulation where the vocal fold motion is not prescribed, but occurs because of interaction with the air, it can be argued that there still will be little effect of the ventricular folds on the oscillation at low frequencies. This is because the vorticity interacting with the negative portion of the gradient of the axial Kirchhoff stream function upstream of the ventricular folds is nearly equal in strength to the vorticity interacting with the positive gradient downstream of the ventricular folds. However, the effect of the ventricular folds on the movement of the vocal folds has not been analyzed here. Further, if the glottal jet strikes the ventricular folds, then their motion would need to be considered.

Similarly, the results presented here may be generalized to fully three-dimensional situations. All that is required is that the changes in vortex strength be small over the regions of nonzero gradients in the axial Kirchhoff stream function that the vorticity traverses.

ACKNOWLEDGMENT

This work was supported by a subaward of Grant No. DC-009299 from the National Institute on Deafness and Other Communication Disorders to the University of California, Los Angeles.

- Agarwal, M. (2004). "The false vocal folds and their effect on translaryngeal airflow resistance." Ph.D. thesis, Bowling Green State University, Bowling Green, OH.
- Agarwal, M., Scherer, R. C., and Hollien, H. (2003). "The false vocal folds: Shape and size in frontal view during phonation based on laminagraphic tracings," *J. Voice* **17**, 97–113.
- Fant, G. (1960). *Acoustic Theory of Speech Production* (Mouton, The Hague, The Netherlands).
- Howe, M. S. (1975). "Contributions to the theory of aerodynamic sound, with application to excess jet noise and the theory of the flute," *J. Fluid Mech.* **71**, 625–673.
- Howe, M. S. (1998). *Acoustics of Fluid-Structure Interactions* (Cambridge University Press, Cambridge).
- Howe, M. S. (2003). *Theory of Vortex Sound* (Cambridge University Press, Cambridge).
- Howe, M. S., and McGowan, R. S. (2007). "Sound generation by aerodynamic sources near a deformable body, with application to voiced speech," *J. Fluid Mech.* **592**, 367–392.
- Lighthill, M. J. (1952). "On sound generated aerodynamically. Part I: General theory," *Proc. R. Soc. London, Ser. A* **211**, 564–587.
- Park, J. B., and Mongeau, L. (2007). "Instantaneous orifice discharge coefficient of a physical, driven model of the human larynx," *J. Acoust. Soc. Am.* **121**, 442–455.
- Rayleigh, L. (1945). *Theory of Sound* (Dover, New York), Vol. 2.
- Stevens, K. N. (1998). *Acoustic Phonetics* (MIT, Cambridge, MA).
- Titze, I. R. (1994). *Principles of Voice Production* (Prentice-Hall, Upper Saddle River, NJ).
- van den Berg, Jw., Zantema, J. T., and Doornenbal, P. (1957). "On the air resistance and the Bernoulli effect of the human larynx," *J. Acoust. Soc. Am.* **29**, 626–631.
- Zhang, C., Zhao, W., Frankel, S. H., and Mongeau, L. (2002). "Computational aeroacoustics of phonation, Part II: Effects of flow parameters and ventricular folds," *J. Acoust. Soc. Am.* **112**, 2147–2154.
- Zhao, W., Zhang, C., Frankel, S. H., and Mongeau, L. (2002). "Computational aeroacoustics of phonation, Part I: Computational methods and sound generation mechanisms," *J. Acoust. Soc. Am.* **112**, 2134–2146.